

Automated Robust Metric Calibration Algorithm for 3D Camera Systems

Christian Heinze*, Stefano Spyropoulos*, Stephan Hussmann[†] and Christian Perwass* *Raytrix GmbH,
Schauenburgerstr. 116, Kiel, Germany

Email: info@raytrix.de [†] Senior Member IEEE, Faculty of Engineering, West Coast University of Applied
Sciences, Heide, Germany
Email: hussmann@fh-westkueste.de

Abstract—The concept of plenoptic cameras has existed since the early 1900s, with recent advances in computational power making them a viable tool for industrial applications. Plenoptic cameras can give 3D information about the scene with one camera, one lens, and a single image. This is possible by placing a microlens array directly in front of the image sensor. The depth estimation is based on disparities observed in individual microlens images, similar to stereo camera approaches. To relate these so-called virtual depth units to metric distances, a camera calibration must be performed. This paper presents a robust, automated camera calibration technique, which introduces new ways to model a multi-focus plenoptic camera.

Keywords - 3D camera system, focused plenoptic, plenoptic 2.0, metric calibration, MLA, Raytrix

I. INTRODUCTION

Stereo vision is widely used and well known for many 3D image applications [1]. A similar approach to Stereo is the light-field measurement approach. The advantage of this approach compared to Stereo is that only one camera with a single lens is needed and all information is captured in a single exposure. A light-field or plenoptic camera acts like a micro camera array that records not only the light intensity but a combination of light intensity and the direction of incident light rays. The plenoptic camera was first described by M. G. Lippmann [2] and before that using pinholes instead of lenses by Ives [3]. The idea was developed further in the past 100 years by many people. More recently the technology was developed further by Ng [4] who built a hand-held plenoptic camera, Levoy [5] who applied the light field technology to microscopy, Georgiev [6] and Lumsdaine [7] who found a way to increase the spatial resolution of plenoptic cameras and Fife [8] who developed a plenoptic CCD sensor. For a more detailed history see Roberts [9]. The images generated by a plenoptic camera have to be processed to obtain a resultant image. The advantages are that in this way the image focus can be varied computationally after the image has been taken. Furthermore, the scene depth can be calculated, which makes a plenoptic camera also a 3D recording device. The price that has to be paid for these additional features is a significant reduction in the effective image resolution.

As mentioned before the 3D depth estimation process of a plenoptic camera works similarly to a stereo camera system and is based on disparities. With a plenoptic camera, it is

possible to generate a light field image and a corresponding depth map concurrently. Once the depth map is known, the intensity image can be refocused to increase the depth of field. The work presented in this paper is created in collaboration with Raytrix GmbH ¹. The plenoptic cameras manufactured by Raytrix deliver the distance from the camera in virtual depth units. A publication detailing the concept of the Raytrix multi-focus plenoptic camera was released in 2012 by Perwass and Wietzke [10].

To allow a precise metric measurement it is not enough to find the relationship between virtual depth and metric depth. It is also necessary to rectify any geometric distortions of the main lens because these would affect the measurements. Previous work in this field has been done by Danserau et al. in 2013 [11]. The paper describes a method to calibrate a Lytro unfocused plenoptic camera. Unfortunately, the Lytro camera is aimed at the consumer market and has so far not been adopted for industrial measurement purposes.

Johannsen et al. provided a first metric calibration for Raytrix plenoptic cameras in [12]. This paper shows that traditional camera calibration algorithms can be applied to plenoptic cameras. The thin lens model is used to project metric depth values from image space into object space. Also, a new distortion model is introduced, which corrects projection errors of a main lens in direction of the optical axis.

Recently a publication was released by Zeller, Quint and Stilla [13], which extends conventional camera calibration techniques to Raytrix plenoptic cameras. This work compares three different methods of calculating metric depth from virtual depth values, going from a physically motivated model to a Taylor approximation of this function. It is again shown that a camera model based on the thin lens equation can be used to obtain metric values from a plenoptic camera.

In comparison to the calibration methods mentioned above, the proposed automated robust metric calibration method introduces a more precise model of the MLA, which not only makes for more precise measurements in 3D space, but also reduces noise in the depth map.

In [14], we presented the first research results of the proposed calibration method. In this manuscript, we have extended the theoretical and the experimental section of the conference paper by introducing a model for the tilt and shift of the main

¹<http://www.raytrix.de>

lens. This new model has been used to generate new result data, using a custom made 3D printed test model as ground truth. This allows for the first time to evaluate the accuracy with just a single image.

The paper is structured as follows. In section II the theoretical background necessary to implement the proposed automated and robust metric calibration method is presented. This includes details about main lens projection, geometric aberrations and the image formation in a plenoptic camera. In section III the implementation of the calibration algorithm is detailed. This includes the design of the calibration target, and the algorithms necessary to perform a robust automated camera calibration. Subsequently in section IV experimental results are given, which show the resolution of a metrically calibrated camera. Finally, a short conclusion and outlook on future work is given in the last section.

II. THEORETICAL FOUNDATIONS

A. Depth estimation

In a plenoptic 2.0 camera like the ones produced by Raytrix, a microlens array is placed directly in front of the image sensor. The placement of this microlens array (MLA) can be seen in figure 1.

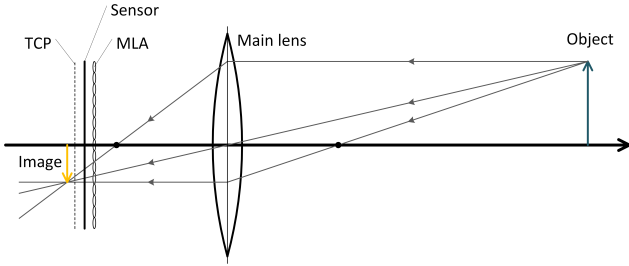


Fig. 1. Schematic drawing of Raytrix plenoptic camera

The total covering plane (TCP) is the plane, on which the main lens must be focused. If the projection of the main lens is any closer to the sensor, no depth estimation is possible. When the MLA is placed in the correct distance from the sensor, the microlenses will project small sub-images onto the sensor. Each of these sub-images shows a slightly different view of the object. When an object point can be seen in at least two sub-images the so called virtual depth of the object point can be estimated. This depth estimation works similarly to stereo vision approaches.

To be able to calculate the virtual depth of a point P_V , the positions i_1 and i_2 of a point pair as seen in two microlenses must be known. For these microlenses, the centers of projection c_1 and c_2 must be known as well. Since only the 2D position of the points on the sensor can be known, the pinhole model is sufficient to project the points behind the sensor and into virtual 3D space. The depth where the two projected rays would intersect in 3D space is the virtual depth v which corresponds to the distance of the object from the camera. A schematic overview of this is given in figure 2.

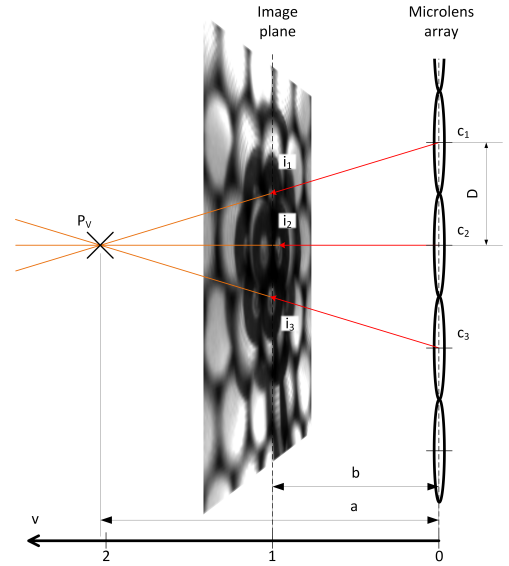


Fig. 2. Schematic drawing of depth estimation principle

These distances are measured in the same direction from the principal plane of the microlens array. Although the distance b is constant but generally not known and a is the metric distance of the projection behind the MLA which shall be found, it is still possible to calculate the virtual depth v . Given the baseline D between c_1 and c_2 and the distance $i_1 - i_2$ between images of the same point in two microlenses, the virtual depth v can be calculated with the intercept theorem (see [12], page 6) :

$$v := \frac{a}{b} = \frac{D}{D - (i_1 - i_2)}. \quad (1)$$

From this equation follows, that to get metric information about the projection behind the MLA, the virtual depth v and the distance from the MLA to the sensor b must be known. This means that the value of b has to be determined by this calibration algorithm.

A unique feature of Raytrix plenoptic cameras is the fact, that they are multi-focus plenoptic cameras. This means that there are three different types of microlenses on an MLA, which differ in their focal length. This design allows for an extended depth of field, yet it can cause a special type of aberration. When an image of a plane target parallel to the sensor is taken, it is expected that there is a single plane of depth estimations in virtual space. Yet measurements have shown that there are actually three distinct planes, one for each type of microlens in the MLA (see figure 3).

The difference in depth between these planes is constant over the image and varies linearly with the virtual depth. Therefore a novel model is proposed, which assumes not one distance b between the MLA and the sensor, but several different values b_i , one for each lens type index b .

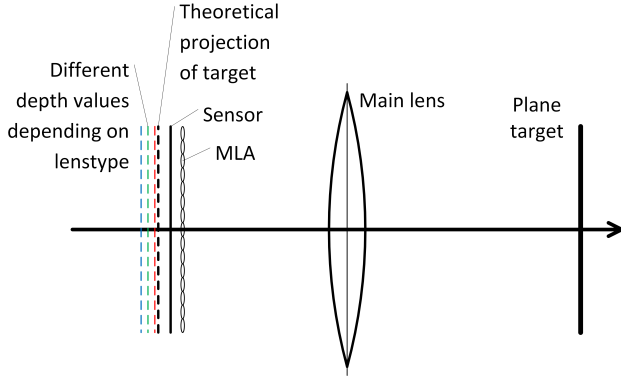


Fig. 3. Multi-focus MLA aberration

B. Projection model

Figure 4 gives an overview of the projection from virtual depth values behind the MLA to metric depth values in front of the camera. The illustration also shows the naming convention for spaces involved in the projection. Points in space I are given in lateral pixel positions on the sensor and virtual depth units. Space II contains points projected from space I into metric coordinates. Points in space III have been undistorted and are given in metric coordinates relative to the principal plane of the main lens. Finally, space IV is located on the other side of the main lens and contains points in the object space. The coordinates of these points are metric, relative to the sensor center. The first step is the projection from virtual depth values

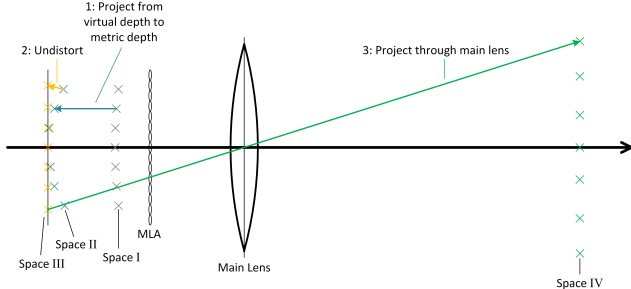


Fig. 4. Projection from virtual depth to metric depth - undistortion - projection through main lens

in space I z_I to metric depth values in space II z_{II} . To calculate this distance, the definition of the virtual depth is used:

$$v := \frac{a}{b_i}. \quad (2)$$

The equation is solved for the metric distance a and the variables are replaced:

$$z_{II} = z_I \cdot b_i. \quad (3)$$

Now each point detected in the target image has a position in 3D space, which can be put into relation with the main lens.

With a 2D camera, it can be helpful to use lateral distortion model of high complexity like e. g. the tangential distortion

model introduced by Brown [15]. With a 2D camera, a tilt or shift of the main lens results in a distorted image on the sensor plane (see figure 5).

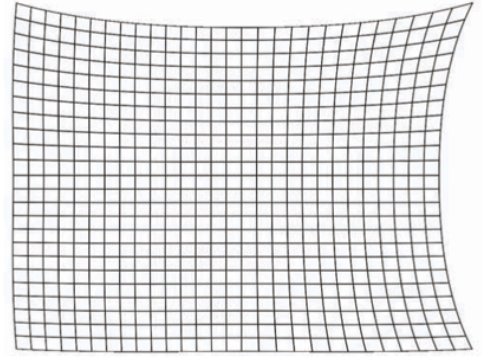


Fig. 5. Effect of tangential distortion caused by lens tilt/shift on a 2D image

With a plenoptic camera, the effect of the lens tilt can be directly observed as a tilt of the 3D image. This effect is known as the Scheimpflug Principle [16], as illustrated in figure 6.

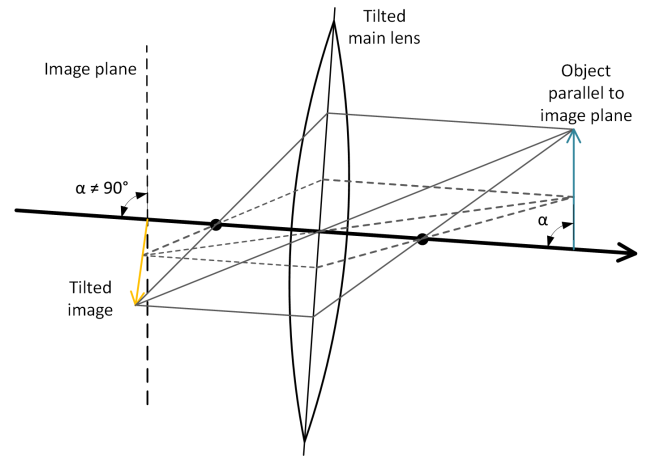


Fig. 6. Effect of lens tilt on a 3D imaging system

We therefore propose to model the tilt and shift of the main lens explicitly in 3D, by describing the full 3D pose of the main lens. This means introducing parameters θ_L , σ_L for the direction of the optical axis of the tilted main lens, along with the parameters X_L , Y_L for the shift of the main lens relative to the sensor center. The distance between sensor and main lens Z_L is already incorporated in this camera model as the image distance B_L (see equation 7).

After any tilt has been removed by applying the model described above, the lateral undistortion model can be applied in a plane perpendicular to the optical axis. The following two equations shift the lateral position of the points to counter radial distortion by applying the method described by Brown [15]. The amount of distortion is controlled through the distortion coefficients k_1 and k_2 . For all these calculations, the radius r is the lateral euclidean distance relative to the

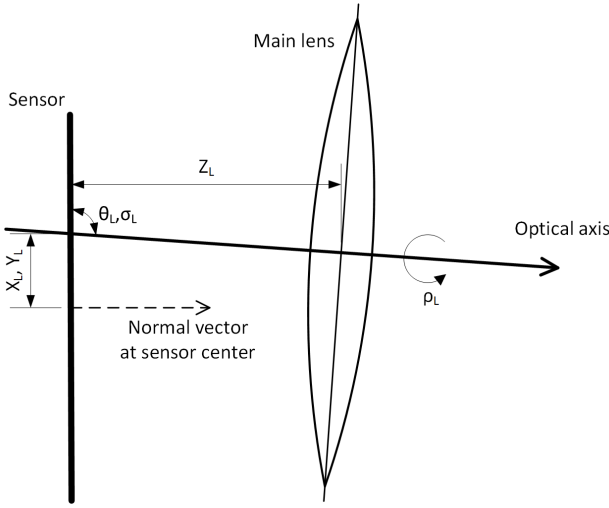


Fig. 7. Model for tilted/shifted main lens

distortion center. The lens distortion is assumed to be radially symmetric around the optical axis, which means the distortion center is known from the parameters X_L, Y_L (see figure 7):

$$x_{III} = x_{II} \cdot (1 + k_1 r^2 + k_2 r^4), \quad (4)$$

$$y_{III} = y_{II} \cdot (1 + k_1 r^2 + k_2 r^4). \quad (5)$$

Following this, the radial depth undistortion is applied. The coefficients d_1 and d_2 model the distortion based on the radius r , while the coefficient d_d models a linear relationship between distortion strength and the virtual depth of a point (compare [12]):

$$z'_{III} = z_{II} + (1 + d_d z_d) \cdot (d_1 r^2 + d_2 r^4). \quad (6)$$

Now the points have been undistorted in lateral and depth directions. The metric depth values are measured from the MLA. To project the points through the main lens, the image distance of each point must be calculated. To do this, the image distance B_L of the main lens must be calculated with the current values of the focal length f_L and the focus distance T_L :

$$B_L = \frac{T_L}{2} \left(1 - \sqrt{1 - 4 \frac{f_L}{T_L}} \right). \quad (7)$$

The image distance is measured from the principal plane of the main lens to the TCP of the plenoptic camera. Therefore, the distance from the TCP to the MLA must be subtracted before adding the metric depth of the points to the image distance:

$$z_{III} = (z'_{III} - 2 \cdot b_i) + B_L. \quad (8)$$

Plenoptic camera design theory states that the distance from the TCP to the sensor is equal to the distance from the sensor to the MLA b_i for the types of plenoptic cameras considered here. This means that the distance from the MLA to the TCP is $2 \cdot b_i$. Subtracting that gives the distance from each point z_{III} to the principal plane of the main lens.

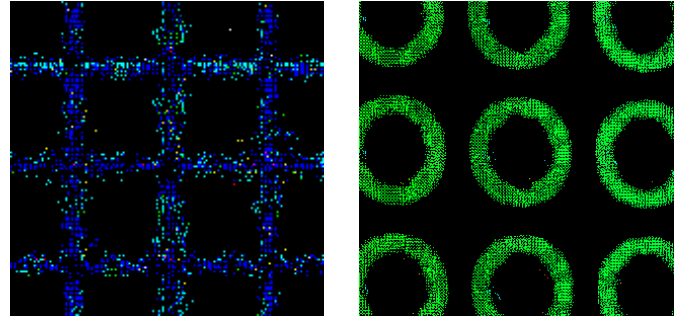


Fig. 8. Targets with linear or circular features

Now the projection through the main lens can be applied. The distance z'_{IV} to which a point is projected in front of the principal plane of the main lens is calculated with the thin lens model:

$$\frac{1}{f_L} = \frac{1}{G_L} + \frac{1}{B_L}. \quad (9)$$

Using the algorithm described in this section, a 3D point from the image given in virtual depths and pixel positions can be projected into metric space in front of the main lens. To find the parameters necessary to perform these calculations, a target based calibration technique is used as described in the next section.

III. IMPLEMENTATION

This chapter comprises not only the implementation of algorithms necessary for the metric calibration of a plenoptic camera, but also details the design of the calibration target. For standard camera calibration techniques, checkerboard targets with known geometry are often used [17]. This type of target can lead to problems with plenoptic cameras, since there are self-similar structures in the image. When an edge of the checkerboard is aligned parallel to an epipolar line of the microlenses, no reliable depth estimation is possible. This can be avoided by using targets with circular features (see figure 8).

To detect the circular features in the total focus image calculated from the light field, the MSER implementation by OpenCV¹ was used. For each 2D position, the virtual depth of the associated point on the target is now extracted (compare figure 8 right).

After this, the 2D pixel positions of the circular features were used as seeds for a custom algorithm, which aligns the features on a rectangular grid and associates the correct metric distances given the feature-pitch on the target. This algorithm is designed with robustness in mind and is described in greater detail in [18].

After this, two sets of point clouds exist. The first cloud consists of the points extracted from the 2D image, with associated virtual depth values (now called target points). The second cloud is comprised of the points aligned on a rectangular grid with a known constant distance between the

¹<http://code.opencv.org/projects/opencv/wiki/MSER>

points (now called model points). There exists a one-to-one mapping from each point detected in the image to a point on the rectangular target model. This relation is now leveraged to perform an optimization of the intrinsic camera parameters.

The target points can now be projected with initial parameters as described in section II-B. The projection of the target points is now located in space IV. Given appropriate initial parameters, these points should lie close to the true position of the target which was held in front of the camera, with close to correct metric positions.

Since the model points lie on a flat target, they are on the sensor plane with $z_{IV} = 0$. An extrinsic pose can now be applied, which shifts the projected target points onto the sensor plane as well.

In this position, the error function of an optimizing algorithm can be calculated. The total number of intrinsic parameters to be optimized is 14. For each image of the target in a different pose, seven parameters for the extrinsic pose are added. Due to the fact that this is a 3D-to-3D calibration, the additional input data makes the calibration quite robust. The recent addition of the full lens pose to the lens model has the potential to decrease the stability of the optimization algorithm. The following results section will address this potential issue and give an measurements of the accuracy that can be achieved.

IV. RESULTS

The goal of this calibration algorithm is to provide a robust automated way to compute a metric calibration for a plenoptic camera. To evaluate the quality of the implementation, it is useful to start with the automatic detection of points in the image and the assignment of model points. This first step not only tests the image processing algorithms, and also makes a statement about the choice of the calibration target type. The focus of the analysis is on precision of the detection and on the robustness of the process. After that, the data gained from the automatic detection should be used to test the optimization step. This again makes both a statement about the implementation of the algorithms, but also about the projection models that were chosen. Indeed, this is a test of the complete calibration algorithm, as the detection and assignment mentioned before also influences the results.

To evaluate the spot detection algorithm and the assignment of the model points, real-world images taken with a Raytrix plenoptic camera are used. The output of the algorithms is visualized by overlaying the calculated coordinates onto the total focus images. First, an ideal case is shown to explain the methodology. Figure 9 shows a total focus image, which was processed by the algorithm. In figure 10, the results of the spot detection and filtering are shown. Note that circles are drawn instead of the ellipses which were actually fitted. These centroid locations are then fed into the algorithm, which assigns the model points and builds the model target coordinate system. Figure 11 shows all locations, for which a model point could be correctly assigned. The larger marker in the middle shows where the center of the target was found. Finally in figure 12, the model points are plotted on a square grid to verify the assignment.

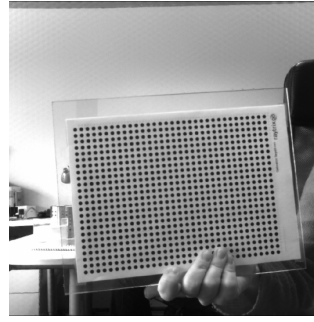


Fig. 9. Total focus image of target

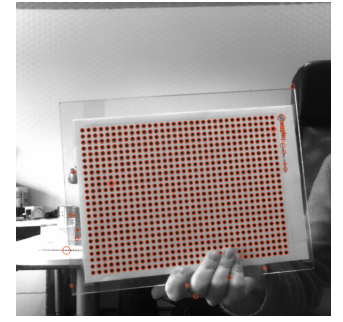


Fig. 10. Spot detection result

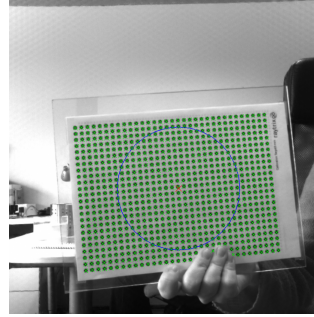


Fig. 11. Target points

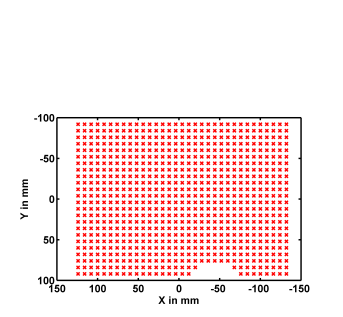


Fig. 12. Model points

This series of images illustrates a typical result of the spot detection and model point assignment algorithms. While the first step of detecting spots still produces some false positives, the second step of aligning the points on a grid leaves only correct points. It should be noted, that the spot detection performs very well, although there is a lot of structure in the background of the image, which could lead to false positive detections. This allows a calibration for larger focus distances, as the target does not have to fill the whole image.

To allow measurements with a plenoptic camera, it is important to evaluate the deviation from known ground truth. To analyze the accuracy, a metric calibration for a camera/lens combination is performed. After that, a plane target is put parallel to the sensor at different metric distances using an automated stage (see figure 13). These distances provide the ground truth. Images of the plane target are taken with the same camera/lens combination. Now the standard depth estimation is performed. Next, the calibration model is applied with the optimized intrinsic parameters, without the newly introduced parameters for the full lens pose. This means that all depth estimations are projected from virtual depth values behind the sensor to metric depth values in front of the camera. The positions in object space should now be as close as possible to the ground truth target distance known for each image.

Figure 14 shows this analysis for a Raytrix R29 camera with a Nikkor 50mm f/1.8 lens focused at 440mm. The upper graph shows the distance from the image or the target to the sensor plotted over the image number. For this analysis, 100 images of the plane target were taken. The target was moved away from the camera from 210mm to a maximum distance of 500mm

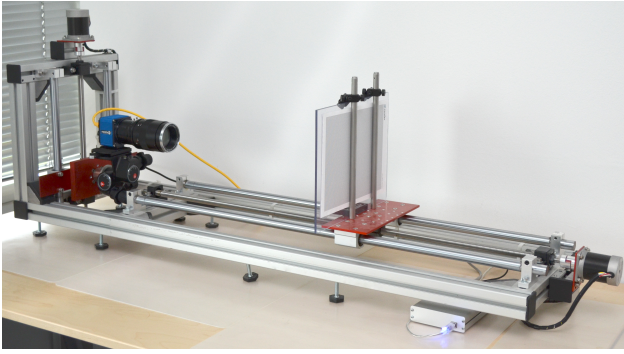


Fig. 13. Automated linear stage for obtaining ground truth data

in steps of $5mm$. The upper plot shows, that the ground truth values and the reprojected values differ by a constant offset. The two lines are parallel to each other over the whole range of depth values. This can also be seen in the lower plot. The error value never drops below $50mm$, but is almost constant over a large part of the depth range. Considering the first 30 images, the distance between ground truth and metric reprojected values is between $58mm$ and $59mm$. Meaning if a constant offset of $58mm$ is added to the metric reprojected values, the distance error is no more than $1mm$ over a large part of the depth range. This constant offset is caused by the use of the thin lens model, which will be replaced by the thick lens model in future versions of the algorithm.

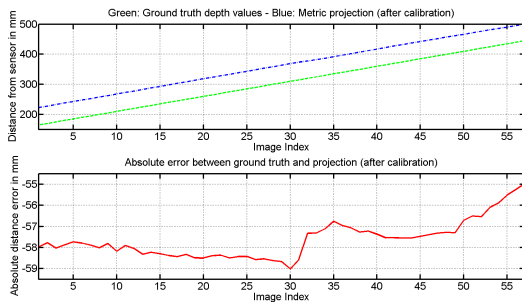


Fig. 14. Error analysis of metric reprojected values for R29 camera

Figure 15 shows the same analysis for a Raytrix R5 camera with a Kowa 25mm $f/2.4$ lens focused at $300mm$. In this case, the error between ground truth and reprojected data is higher. This is due to the fact, that the R5 camera has less depth resolution than the R29 camera. Yet this case demonstrates, that it is possible to measure absolute distances from the camera.

Future analysis will focus on measuring the standard deviation of the reprojected data in metric space.

Yet first, the effectivity of the newly introduced offsets b_i for the MLA-Sensor distance is tested. To do this, calibrations were performed for an R5 camera with a Kowa 50mm $f/2.4$ lens focused at $500mm$. In the first calibration, only one MLA-Sensor distance b was estimated. This corresponds to the camera model described in [12].

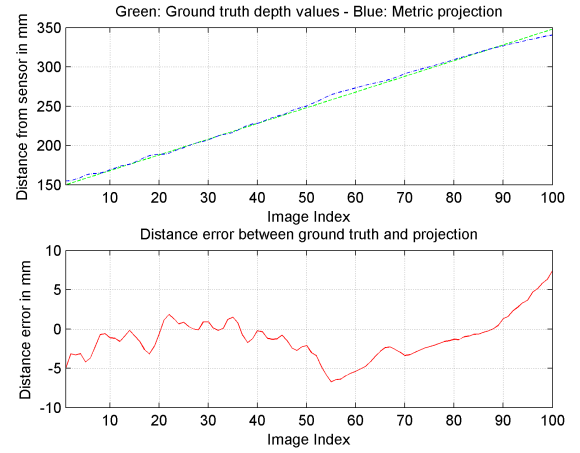


Fig. 15. Error analysis of metric reprojected values for R5 camera

TABLE I. METRIC DEPTH VALUES OF REPROJECTED PLANE TARGET WITH AND WITHOUT CORRECTION FOR MLA ABERRATION

Lens type	Correction off absolute depth	Correction off relative error	Correction on absolute depth	Correction on relative error
Far	616.3255	0%	592.3340	0%
Middle	612.5430	-0.62%	590.4700	-0.32%
Near	609.4920	-1.12%	590.3000	-0.34%

For the second calibration, three values b_i were used in the calibration process. After that, a plane target was placed at a distance from the sensor where all three lens types produce valid depth estimations. The depth values for this target were reprojected to metric space in front of the camera. The desired result is that the points in metric space form a plane. Yet table I shows, that without correction, the projection results in three planes at different distances from the sensor. The distance values were obtained by fitting a plane to the point cloud and evaluating the value in the center.

The percentage errors are calculated relative to the plane projected from the data of the far lens type. When looking at the relative error with the new correction method introduced in this paper, it can be seen that the distance between the planes has been reduced compared to before. For example, points with depth estimations from the middle and near lens type would now just lie $0.17mm$ apart, while this error without correction would be over $3mm$. If a systematic error of $3mm$ exists for depth estimations of the same point of the object with different lens types, reducing this error will greatly reduce the noise of the resulting depth map of the object.

As mentioned above, all previous calibration results were obtained without using the newly introduced model for the full lens pose. For the final test, the new model was incorporated to test the calibration reliability and accuracy with a 3D printed object with known ground truth. Figure 16 shows a 2D image of this object. Since the exact dimensions of the object are known, the accuracy of the metrically calibrated camera system can be evaluated with just one image. The object measures $50mm \times 50mm \times 25mm$ and features a series of steps

with precisely known heights, along with three plane features located at 45 degree angles to each other.

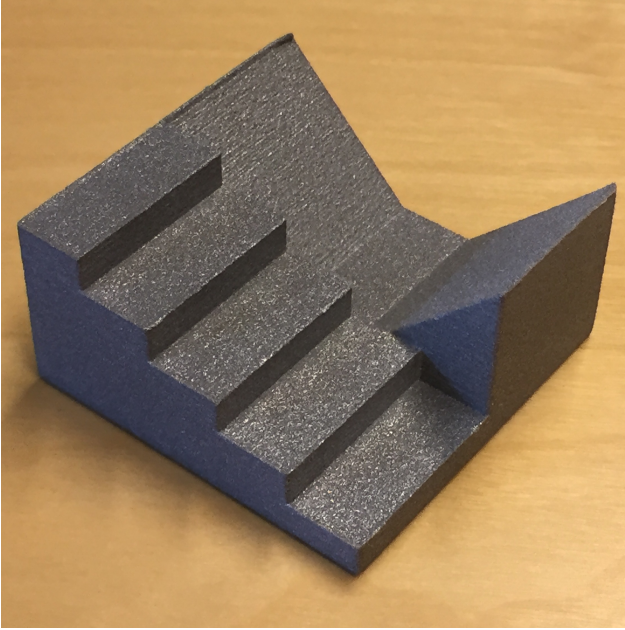


Fig. 16. 3D-printed object with known ground truth for accuracy analysis

The image was taken with an R29 camera with a Zeiss 100mm f/2.0 lens focused at 500mm. The robustness of the optimization algorithm has not been negatively affected by introducing the full model for the lens pose. The calibration for this setup has converged at the first test with only four target images used for the calibration. Figure 17 shows the output of the metric calibration as a point cloud of values which were then used to analyze the accuracy.

The accuracy analysis consists of two measurements. First, the height differences for the series of steps is evaluated. The steps are detected in the image and a plane is fit to each step using a RANSAC algorithm. Table II shows the measurement results.

TABLE II. ACCURACY ANALYSIS FOR STEP SERIES

	Step 1	Step 2	Step 3	Step 4	Step 5
Distance from Camera (mm)	436.05	441.07	445.93	450.79	455.45
Step Height (mm)	0	5.02	4.86	4.86	4.65
Ground Truth Step Height (mm)	0	5	4.95	5	4.95
Step Height Error (mm)		0.02	0.09	0.14	0.30

The values for the step height errors show, that the optimization has not only converged, but has resulted in a good set of intrinsic camera parameters. This result compares favorably to the results shown in figure 14, where higher error values were present even though image-filling noise targets were used to generate each single depth value for analysis. In this test, one image is taken with the camera and only small parts of the image are evaluated and related to each other. This test is much closer to the actual applications for which these cameras

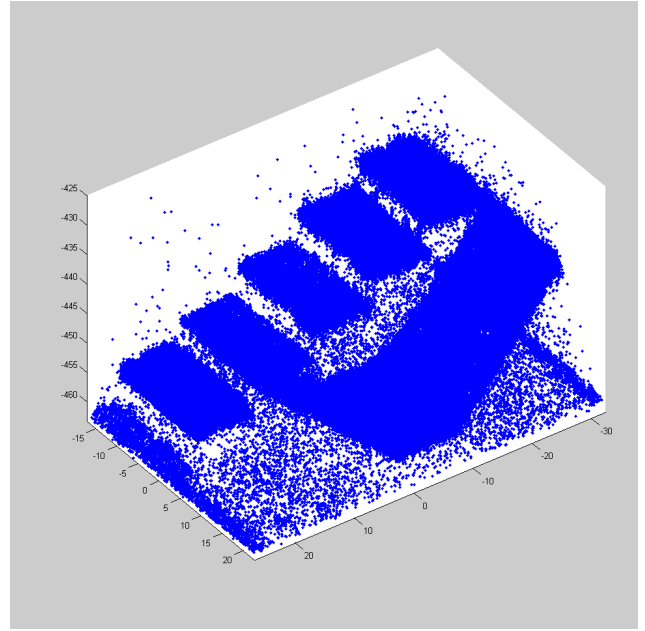


Fig. 17. Point cloud of depth estimations for 3d printed object with known ground truth

are used, and still shows a very high accuracy. It should be noted that the step height error values increase monotonically as the steps get closer to the camera, so there is still room for improvement.

V. CONCLUSION

We have presented a method of metrically calibrating a multi-focus plenoptic camera. This work introduces a method to rectify aberrations introduced by the MLA of this type of camera. Further, a new physically based model for correcting lens distortions by estimating the pose of the lens has been incorporated.

As the results in section IV above show, this implementation allows modeling a plenoptic camera with a main lens accurately, so that a metric calibration can be performed. It has been shown that the calibration process is very robust. Calibrations were performed for many different cameras, lenses and lens settings. No special care was taken with regard to the images of the calibration targets. The lighting, pose and scale of the targets varied greatly from shot to shot, yet all calibration processes have converged to a plausible set of parameters. The detection algorithms performed good, while not introducing any false positive points. Finally, the newly introduced correction for MLA aberration and the depth undistortion have produced the expected results. This means that this implementation is fit to be incorporated into the Raytrix RxLive software package. The next chapter will give an outlook to further possibilities and sums up this work.

We plan to further extend this calibration technique, by adopting the thick lens model should be the projection, which would allow the calibration of extreme macro lenses and microscopes. This will include a new approach to obtaining the

target images. Further, there are plans to use this calibration technique in a multi camera system approach together with 2D cameras, laser scanners and time of flight cameras. The final step would be to extend the calibration to use the raw image as recorded by the camera sensor. This would allow the calibration of individual microlenses, which could further reduce systematic noise in the depth estimation. The current release of the Raytrix RxLive software uses a projection model and metric calibration system based on this work. This software is already in use at customers, and the feedback has been very good.

REFERENCES

- [1] Faugeras, O.: *Three-Dimensional Computer Vision: A Geometric View-point*. MIT Press, Cambridge, Massachusetts, 1993.
- [2] Lippmann, G.: *Epreuves reversibles, photographies integrals*. Academie des sciences , 446451, 1908.
- [3] Ives, F.: *Parallax Stereogram and Process of Making Same*. United States Patent Application 725,567, 1902.
- [4] Ng, R.; Levoy, M., Bredif, M., Duval, G., Horowitz, M. and Hanrahan, P.: *Light Field Photography with a Hand-Held Plenoptic Camera*. Stanford University Computer Science Tech Report CSTR 2005-02, (Online) <http://graphics.stanford.edu/papers/lfcamera/> (accessed 12/2014), 2005.
- [5] Levoy, M., Ng, R., Adams, A., Footer, M. and Horowitz, M.: *Light field microscopy*. ACM Trans. Graph., 25(3), 924934, 2006.
- [6] Georgiev, T. and Intwala, C.: *Light-field camera design for integral view photography*. Tech. rep., Adobe Systems, Inc., 2006.
- [7] Lumsdaine, A. and Georgiev, T.: *Full resolution lightfield rendering*. Tech. rep., Adobe Systems, Inc., 2008.
- [8] Fife, K., Gamal, A. E., and Wong, H.-S. P.: *A 3mpixel multi-aperture image sensor with 0.7um pixels in 0.11um cmos*. IEEE ISSCC Digest of Technical Papers, pp. 4849, 2008.
- [9] Roberts, D. E.: *History of lenticular and related autostereoscopic methods*. Leap Technologies, LLC, 2003.
- [10] Perwass, C., Wietzke, L.: *Single lens 3D camera with extended depth-of-field*, Proc. SPIE 8291, Human Vision and Electronic Imaging XVII, 2012.
- [11] Danserau, D., Pizarro, O. Williams, S.: *Calibration and rectification for lenselet-based plenoptic cameras*, Proc. International Conference on Computer Vision and Pattern Recognition, 2013.
- [12] Johannsen, O. et al.: *On the Calibration of Focused Plenoptic Cameras* http://hci.iwr.uni-heidelberg.de/Staff/bgoldlue/papers/JHGPI3_gcpr_inm.pdf [15.09.14].
- [13] Zeller, N., Quint, F., Stilla, U.: *Kalibrierung und Genauigkeitsuntersuchung einer fokussierten plenoptischen Kamera*, DGPF Tagungsband 23, 2014.
- [14] Heinze, C. et al.: *Automated Robust Metric Calibration of Multi-Focus Plenoptic Cameras* in Proc. of the 32nd Int. Conf. on Inst. and Meas. Tec., IEEE Instrumentation and Measurement Society, 2038-2043, 2015.
- [15] Brown, D. C.: *Decentering distortion of lenses*, Photometric Engineering 32(3), 444-462, 1966.
- [16] Scheimpflug, T.: *Improved Method and Apparatus for the Systematic Alteration or Distortion of Plane Pictures and Images by Means of Lenses and Mirrors for Photography and for other purposes*, GB Patent No. 1196. Filed 16 January 1904, and issued 12 May 1904
- [17] Tsai, R. Y.: *A Versatile Camera Calibration Technique for High-Accuracy 3D Machine Vision Metrology Using Off-the-shelf TV Cameras and Lenses*, IEEE Journal of Robotics and Automation, Vol. RA-3, No. 4, August 1987.
- [18] Heinze, C.: *Design and test of a calibration method for the calculation of metrical range values for 3D light field cameras*, Master's thesis, 98 pages, West Coast University of Applied Sciences, Heide, Germany, 2014.



Christian Heinze Christian Heinze received his Master of Science in Microelectronic Systems in 2014 from a joint study programme at the Fachhochschule Westkste - University of Applied Sciences, Heide, Germany and the Hamburg University of Applied Sciences, Hamburg, Germany. He joined Raytrix for his master's thesis in 2013, and received the Fokusfinder 2014 award for best thesis in the area of industrial image processing in the UV/VIS/IR spectrum. He is currently an application engineer in the research and development department at Raytrix GmbH. His research interests include light field camera technology, metric calibration of light field cameras, and manufacturing methods for light field cameras.



Stefano Spyropoulos Stefano Spyropoulos received the diploma degree in computer science from Christian-Albrechts-University, Kiel, Germany, in 2013. He joined Raytrix GmbH in 2014 and is currently a software engineer in the research and development department. His current research interests include lightfield camera image processing and metric calibration of lightfield cameras.



Stephan Hussmann Stephan Hussmann (SM'11) received his M.E. and Ph.D. degrees from the University of Siegen, Siegen, Germany, in 1995 and 2000, respectively. From 1996 to 2000, he was a Research Associate with the Center for Sensor Systems (ZESS), University of Siegen, and a Development Engineer with Aicoss GmbH, Siegen. From 2001 to 2003, he was a Lecturer with the Department of Electrical and Computer Engineering, University of Auckland, Auckland, New Zealand. Since the end of 2004, he has been a Professor with the Faculty of Engineering, West Coast University of Applied Sciences (FWH), Heide, Germany, in the area of microprocessor technology and electronic systems. He has widely consulted with the industry and has more than 60 publications, which include book chapters, international patents, and refereed journal and conference proceedings papers. His research interests include low-cost multi-sensor system design, real-time 2D/3D image processing and embedded systems design.



Christian Perwass Christian Perwass received his Ph.D. in engineering from Cambridge University, UK and his habilitation in Computer Science from Kiel University, Germany. He then worked in R&D at Robert Bosch GmbH developing automated optical inspection systems before founding the company Raytrix GmbH to develop and market 3D light field cameras for research and industrial applications. He is author of a book on Geometric Algebra and developed the award winning multi-focus plenoptic camera, which became a unique enabling technology for a number of applications in research and industry.